THEORETICAL AND APPLIED MECHANICS
24, pp. 29-54, 1998, UDK 536.24

A mathematical model and numerical solution for the conjugated heat transfer in a fully partitioned enclosure containing the fluids with variable nonlinear thermophysical properties

Dušanka M. Čučković-Džodžo
Milorad B. Džodžo and Miloš D. Pavlović

Submitted 21 April 1997

Abstract

Laminar natural convection in an enclosure divided by a complete vertical conducting partition is studied numerically by using a stationary two dimensional model. Two opposite vertical sides of the enclosure were at constant different temperatures. The working fluid was glycerol. The heat conducting partition was positioned in the middle of the enclosure. The governing equations with variable density and thermophysical characteristics of the fluid were used. An appropriate finite volume numerical procedure based on SIMPLE, uniform collocated grid and deferred correction central difference scheme for convective terms has been developed. Numerical procedure was verified by comparing the results with numerical bench mark solutions for a cavity without partition filled with air and also by comparing them with the available experimental results for a partitioned cavity filled with glycerol. The developed procedure

takes into account the nonlinear dependence of the thermophysical characteristics of the glycerol (especially viscosity) so that a better agreement with the experimental results was achieved.

1 Introduction

Natural convection in enclosures has been receiving considerable attention in past decades. This is due to a lot of its applications such as in solar collectors, thermal design of buildings, nuclear reactor design and so on.

The problem of the laminar natural convection in enclosures with partitions was treated experimentally by Duxbury, 1979, where the working fluid was air; Anderson and Bejan, 1981; Nishimura et al., 1988, with water as working fluid and Nakamura et al., 1984, with the radiation effects included as well.

The same problem was investigated analytically and numerically by Anderson and Bejan, 1981; Nakamura et al., 1984; Acharya and Tsang, 1985; Tong and Gerner, 1986; Ho and Yih, 1987; Nishimura et al., 1988; Kangni et al., 1991; Ciofalo and Karayiannis, 1991; Karayiannis et al., 1992; and Mamou et al., 1994. In most of the papers the fluid used was air (Pr=0.71), but in some cases water was used as well. The Bussinesq approximation was used for all numerical models, and it is justifiable if the density is linearly dependent on temperature and other properties of the fluid are assumed to be constant. These assumptions are valid if air and water are the working fluids, and temperature differences of the opposite sides of the cavity are small.

In this paper glycerol was used as a working fluid. The coefficient of the dynamic viscosity of glycerol depends nonlinearly on the temperature and thus can decrease by an order of magnitude between the different temperatures of the opposite walls. Therefore, to obtain a better agreement between the experimental and numerical results, the equations with variable properties of fluid were used. To increase numerical accuracy, the convective terms were approximated by using the deferred correction central difference scheme and a uniform grid.

2 Numerical method

2.1 Governing equations

A two dimensional numerical simulation of natural convection was performed. The steady state equations for the fluid with variable properties were used in the mathematical model. The continuity and momentum equations read

$$\frac{\partial}{\partial x}\rho u + \frac{\partial}{\partial y}\rho v = 0, \tag{1}$$

$$\frac{\partial}{\partial x}\rho uu + \frac{\partial}{\partial y}\rho vu = \frac{\partial}{\partial x}[2\mu\frac{\partial u}{\partial x} - \frac{2}{3}\mu(\nabla V)] + \frac{\partial}{\partial y}[\mu(\frac{\partial u}{\partial y} + \frac{\partial v}{\partial x})] - \frac{\partial p}{\partial x}, \tag{2}$$

$$\frac{\partial}{\partial x}\rho uv + \frac{\partial}{\partial y}\rho vv = \frac{\partial}{\partial x}[\mu(\frac{\partial v}{\partial x} + \frac{\partial u}{\partial y})] + \frac{\partial}{\partial y}[2\mu\frac{\partial v}{\partial y} - \frac{2}{3}\mu(\nabla V)] - \frac{\partial p}{\partial y} + \rho g, \tag{3}$$

The energy equation for the fluid is

$$\frac{\partial}{\partial x}\rho u c_p T + \frac{\partial}{\partial y}\rho v c_p T = \frac{\partial}{\partial x}(k_f\frac{\partial T}{\partial x}) + \frac{\partial}{\partial y}(k_f\frac{\partial T}{\partial y}), \tag{4}$$

while the energy (conduction) equation for the partition wall reads

$$\frac{\partial}{\partial x}(k_p\frac{\partial T}{\partial x}) + \frac{\partial}{\partial y}(k_p\frac{\partial T}{\partial y}) = 0. \tag{5}$$

The boundary conditions are presented in Figure 1. The horizontal walls were assumed to be adiabatic, while the vertical walls were maintained at constant different temperatures. The conjugate heat transfer

boundary conditions were applied for the vertical partition.

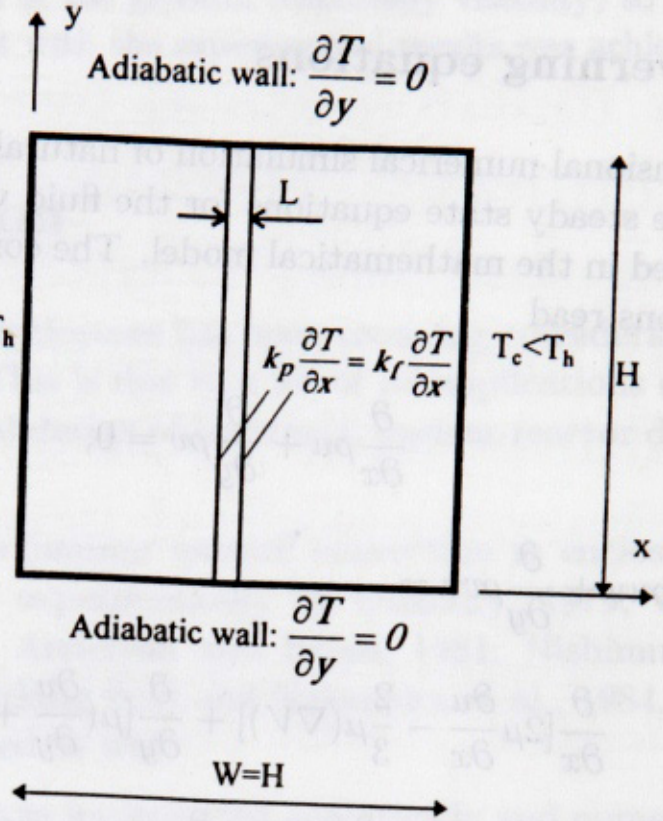

Fig. 1. Physical model of the fully partitioned enclosure.

The dimension of the enclosure was 38 x 38 x 38 mm. The partition was made of Plexiglas, 2mm thick. The partition was placed midway between the vertical walls.

The momentum equations (2) and (3) can be written in a form similar to that of energy equation (4), i. e.

$$\frac{\partial}{\partial x}\rho uu + \frac{\partial}{\partial y}\rho vu = \frac{\partial}{\partial x}(\mu\frac{\partial u}{\partial x}) + \frac{\partial}{\partial y}(\mu\frac{\partial u}{\partial y}) - \frac{\partial p}{\partial x} + B_x + V_x, \quad (6)$$

and

$$\frac{\partial}{\partial x}\rho uv + \frac{\partial}{\partial y}\rho vv = \frac{\partial}{\partial x}(\mu\frac{\partial v}{\partial x}) + \frac{\partial}{\partial y}(\mu\frac{\partial v}{\partial y}) - \frac{\partial p}{\partial y} + B_y + V_z, \quad (7)$$

where

$$B_x = \rho g_x = 0, \quad B_y = \rho g_y = \rho g, \tag{8}$$

are buoyancy volumetric forces, and

$$V_x = \frac{1}{3}\frac{\partial}{\partial x}(\mu\frac{\partial u}{\partial x}) + \frac{\partial}{\partial y}(\mu\frac{\partial v}{\partial x}) - \frac{2}{3}\frac{\partial}{\partial x}(\mu\frac{\partial v}{\partial y}), \tag{9}$$

$$V_y = \frac{1}{3}\frac{\partial}{\partial y}(\mu\frac{\partial v}{\partial y}) + \frac{\partial}{\partial x}(\mu\frac{\partial u}{\partial y}) - \frac{2}{3}\frac{\partial}{\partial y}(\mu\frac{\partial u}{\partial x}), \tag{10}$$

are additional terms related to the viscosity.

For an incompressible fluid (ρ = constant) and fluid with constant viscosity (μ = constant) V_x and V_z become zero. The assumption of the density to be linearly dependent on the temperature only in equations (8), in fact the application of the Boussinesq approximation, opens the way to take into account the influence of the buoyancy forces on the natural convection. The assumptions mentioned were applied also in the most of the previous natural convection numerical models where the working fluids were air and water.

In this paper, Boussinesq approximation is not applied and the fluid properties are functions of temperature (defined as additional set of algebraic equations). As a consequence, members (9) and (10) in the momentum equations (6) and (7) are to be taken into account.

2.2 Discretization of the governing equations

To discretize the domain and derive difference equations, the control volume method based on the finite difference approach was used. Uniform collocated grid (Fig. 2) was applied for all variables - components of velocities, pressure and temperature. The numbers of control volume cells were 76, 36 and 8 in the vertical direction, in the horizontal direction in each half of the enclosure and in the horizontal direction

for the partition, respectively.

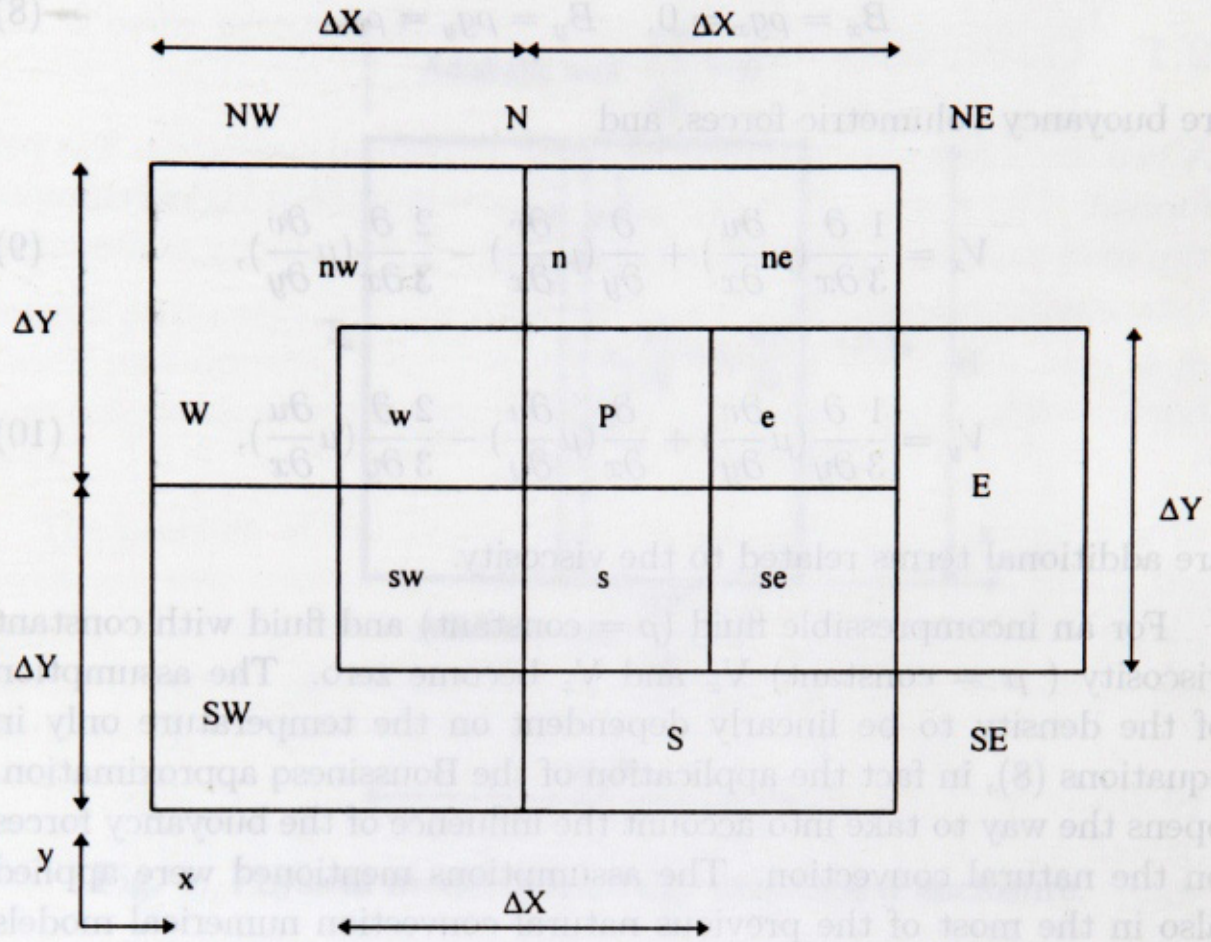

Fig. 2. Control volume cell.

The terms in the momentum equations like $(-\partial p/\partial x + B_x + V_x$ and $-\partial p/\partial y + B_z + V_z)$ are present as source terms in the finite difference equations, so that the form and derivation of the finite difference momentum equations are similar to those of the energy equation (see Patankar, 1980).

The finite difference equations were derived by using the central difference scheme for both convective and diffusive terms. To obtain the convergence of the numerical procedure, the central difference scheme for the convective terms is used with the "deferred correction" as in (Khosla and Rubin, 1974). The details of the finite difference derivations which are different from the procedures in (Patankar, 1980) will be presented here.

By using the second order central difference scheme (see Fig. 2) the equation (6) could be written in the following finite difference form:

$$\frac{\rho_e U_e \frac{U_E + U_P}{2} - \rho_w U_w \frac{U_P + U_W}{2}}{\Delta X} + \frac{\rho_n V_n \frac{U_N + U_P}{2} - \rho_s V_s \frac{U_P + U_S}{2}}{\Delta Y} =$$

$$\frac{\mu_e \frac{U_E - U_P}{\Delta X} - \mu_w \frac{U_P - U_W}{\Delta X}}{\Delta X} + \frac{\mu_n \frac{U_N - U_P}{\Delta Y} - \mu_s \frac{U_P - U_S}{\Delta Y}}{\Delta Y} - \frac{P_e - P_w}{\Delta X} +$$

$$+\frac{1}{3}\frac{\mu_e \frac{U_E - U_p}{\Delta X} - \mu_w \frac{U_P - U_W}{\Delta X}}{\Delta X} + \frac{\mu_n \frac{Vne - V_{nw}}{\Delta X} - \mu_s \frac{V_{se} - V_{sw}}{\Delta X}}{\Delta Y} -$$

$$-\frac{2}{3}\frac{\mu_e \frac{Vne - V_{se}}{\Delta Y} - \mu_w \frac{V_{nw} - V_{sw}}{\Delta Y}}{\Delta X}, \tag{11}$$

If the first order upwind scheme is used for the convective terms, the left side of the equation (11) takes the form

$$AMAX1(\rho_w U_w, 0)\frac{(U_P - U_W)}{\Delta X} + AMIN1(\rho_e U_e, 0)\frac{(U_E - U_P)}{\Delta X} +$$

$$+AMAX1(\rho_s V_s, 0)\frac{(U_P - U_S)}{\Delta Y} + AMIN1(\rho_n V_n, 0)\frac{(U_N - U_P)}{\Delta Y}, \tag{12}$$

as in (Patankar, 1980), where $AMAX1$ and $AMIN1$ are FORTRAN functions defining maximal or minimal values of the attributes.

If we add expression (12) to both sides of the equation (11) and multiply it by $\Delta X \Delta Y$, then the finite difference equation is obtained

$$A_P U_P = A_W U_W + A_E U_E + A_S U_S + A_N U_N + S_U, \tag{13}$$

where:

$$A_W = \mu_w \Delta Y / \Delta X + AMAX1(\rho_w \Delta Y U_w, 0), \tag{14}$$

$$A_E = \mu_e \Delta Y/\Delta X - AMIN1(\rho_e \Delta Y U_e, 0), \tag{15}$$

$$A_S = \mu_s \Delta X/\Delta Y + AMAX1(\rho_s \Delta X V_s, 0), \tag{16}$$

$$A_N = \mu_n \Delta X/\Delta Y - AMIN1(\rho_n \Delta X V_n, 0), \tag{17}$$

$$A_P = A_W + A_E + A_S + A_N, \tag{18}$$

$$S_U = S_U^P + S_U^B + S_U^{VIS} + S_U^D, \tag{19}$$

$$S_U^P = -\Delta Y(P_e - P_w), \tag{20}$$

$$S_U^B = \Delta X \Delta Y \rho g_x, \tag{21}$$

$$S_U^{VIS} = \frac{1}{3}\left[\mu_e(U_E - U_P) - \mu_w(U_P - U_W)\right]\frac{\Delta Y}{\Delta X} + \mu_n(V_{ne} - V_{nw}) -$$
$$-\mu_s(V_{se} - V_{sw}) - \frac{2}{3}[\mu_e(V_{ne} - V_{se}) - \mu_w(V_{nw} - V_{sw})], \tag{22}$$

$$S_U^D = -\rho_e U_e \Delta Y \frac{(U_E + U_P)}{2} + \rho_w U_w \Delta Y \frac{(U_P + U_W)}{2} -$$
$$-\rho_n V_n \Delta X \frac{(U_N + U_P)}{2} + \rho_s V_s \Delta X \frac{(U_P + U_S)}{2} +$$
$$+AMAX1(\rho_w U_w \Delta Y, 0) \cdot (U_P - U_W) + \tag{23}$$
$$+AMIN1(\rho_e U_e \Delta Y, 0) \cdot (U_E - U_P) +$$
$$+AMAX1(\rho_s V_s \Delta X, 0) \cdot (U_P - U_S) +$$
$$AMIN1(\rho_n V_n \Delta X, 0) \cdot (U_N - U_P).$$

To note is that the coefficients A_W, A_E, A_S, A_N (14-17) are the same as if the first order upwind scheme (see Patankar, 1980) is used for the convective terms. The influence of the central difference scheme is presented in the part of the source term S_U^D (23) which represents the difference between the central and upwind difference schemes terms (as in (Khosla and Rubin, 1974)). By doing so the second order accuracy (due to the grid being uniform) and the stability of the numerical procedure were obtained.

To obtain the velocities U_w, U_e, V_n, V_s and fluxes on the faces of the collocated control volume cells, the interpolation of the momentum equations were used as in (Rhie,1981).

The calculation of the coefficients A_W, A_E, A_S, A_N in equation (13) as well as of the source term S_U is based on the values of the velocities, pressures, temperatures and thermophysical properties of the fluid in the previous iteration of the numerical procedure SIMPLE (Patankar and Spalding, 1972).

The modified equation (20) is used to calculate Up

$$U_P = \frac{A_W U_W + A_E U_E + A_S U_S + A_N U_N + S_U + \frac{1-\alpha_u}{\alpha_u} A_P U_P^*}{\frac{A_P}{\alpha_u}}, \quad (24)$$

where α_u and U_p^* are the factor of underrelaxation (in this case, $\alpha_u = \alpha_v = 0.8$) and the value from the previous iteration of the SIMPLE procedure, respectively. The system of the algebraic equations is solved iteratively by using the procedure (Stone, 1968) as in (Peric, 1985).

The system of finite difference equations for the vertical velocity components and temperature are derived in a similar way. The only difference is that the finite difference equation for temperature (25) (with $T = 0.8$) has an additional factor G multiplying the source term S_U^T presenting the difference between the central and upwind difference scheme terms and thus yielding

$$T_P = \frac{A_W^T T_W + A_E^T T_E + A_S^T T_S + A_N^T T_N + G \cdot S_U^T + \dfrac{1-\alpha_T}{\alpha_T} A_P^T T_P^*}{\dfrac{A_P^T}{\alpha_T}}. \tag{25}$$

To obtain the stability of the overall SIMPLE numerical procedure at the beginning of the calculation, the upwind scheme was used for the convective terms in the energy equation (by using $G = 0$). After a prescribed number of SIMPLE iterations the central difference scheme was introduced ($G = 1$) to provide (retain) the second order accuracy.

The flow and temperature fields were first solved in the portion of the enclosure near the hot wall, then the temperature distribution inside the partition was obtained, and finally the flow and temperature fields inside the portion of the enclosure near the cold wall were found. The procedure used to be repeated until the convergence of the solution was reached. The convergence criterion was based on the average mass imbalance to be less than 10^{-9}.

3 Verification of the numerical procedure

3.1 Comparison of the numerical results for the unpartitioned enclosure filed with air

To verify the applied numerical procedure, the results for a cubic enclosure without partition were compared with the benchmark results presented by (de Vahl Davis, 1983) and (Hortmann M., et al. 1990).

Two vertical opposite walls were maintained at constant different temperatures and the horizontal walls were assumed to be adiabatic. The working fluid was air ($Pr = 0.71$). The comparison was performed for the Rayleigh numbers $Ra = 10^4$, $Ra = 10^5$ and $Ra = 10^6$. The results presented by (de Vahl Davis, 1983) and (Hortmann M., et al. 1990) were obtained by using 81 x 81 and 640 x 640 grids, respectively.

In both papers the Boussinesq approximation was used. The density was linearly dependent on temperature only in the buoyancy force term while the thermophysical properties of air were considered to be constant. For small temperature differences between the opposite vertical walls, the application of the Boussinesq approximation for air is justifiable.

To verify the numerical model with variable thermophysical properties, the following expressions for air properties were used

$$\rho = -4.167 \cdot 10^{-11} \cdot T_C^5 + 1.0 \cdot 10^{-8} \cdot T_C^4 - 9.625 \cdot 10^{-7} \cdot T_C^3 + \\ +5.7 \cdot 10^{-5} \cdot T_C^2 - 5.563 \cdot 10^{-3} \cdot T_C + 1.299 \ [kg/m^3], \tag{26}$$

$$\mu = -1.772 \cdot 10^{-27} \cdot T_C^5 - 8.333 \cdot 10^{-14} \cdot T_C^4 + 1.5 \cdot 10^{-11} \cdot T_C^3 - \\ -9.917 \cdot 10^{-10} \cdot T_C^2 + 7.45 \cdot 10^{-8} \cdot T_C + 1.697 \cdot 10^{-5} \ [kg/ms], \tag{27}$$

$$k = -4.285 \cdot 10^{-8} \cdot T_K^2 + 9.878 \cdot 10^{-5} \cdot T_K + 3.675 \cdot 10^{-4} \ [W/mK], \tag{28}$$

$$c_p = -5.555 \cdot 10^{-6} \cdot T_K^3 + 5.802 \cdot 10^{-3} T_K^2 - 1.95 \cdot T_K + 1.219 \cdot 10^3 \ [J/kgK], \tag{29}$$

$$\beta = 3.393 \cdot 10^{-8} \cdot T_C^2 - 1.306 \cdot 10^{-5} \cdot T_C + 3.659 \cdot 10^{-3} \ [1/K]. \tag{30}$$

The expressions (26-30) for air properties are based on the data from (Schmidt F.W. et al., 1993) and can be applied for the temperature range 20-60^oC.

The temperatures of the vertical sides were 21.77 - 20^oC, 40.36 - 20^oC and 46.7 - 20^oC, to provide the results corresponding to $Ra = 10^4$, $Ra = 10^5$ and $Ra = 10^6$, respectively. For the last case ($Ra = 10^6$) the size of the enclosure was increased from 38 mm to 76 mm (so that

the set of equations (26-30) for the same temperature range were used). All calculations were performed by using a uniform grid with 76 x 76 control volume cells. The streamlines and isotherms for $Ra = 10^4$, $Ra = 10^5$ and $Ra = 10^6$ (Fig. 3) were compared with those from (de Vahl Davis G., 1983) and a good agreement was achieved.

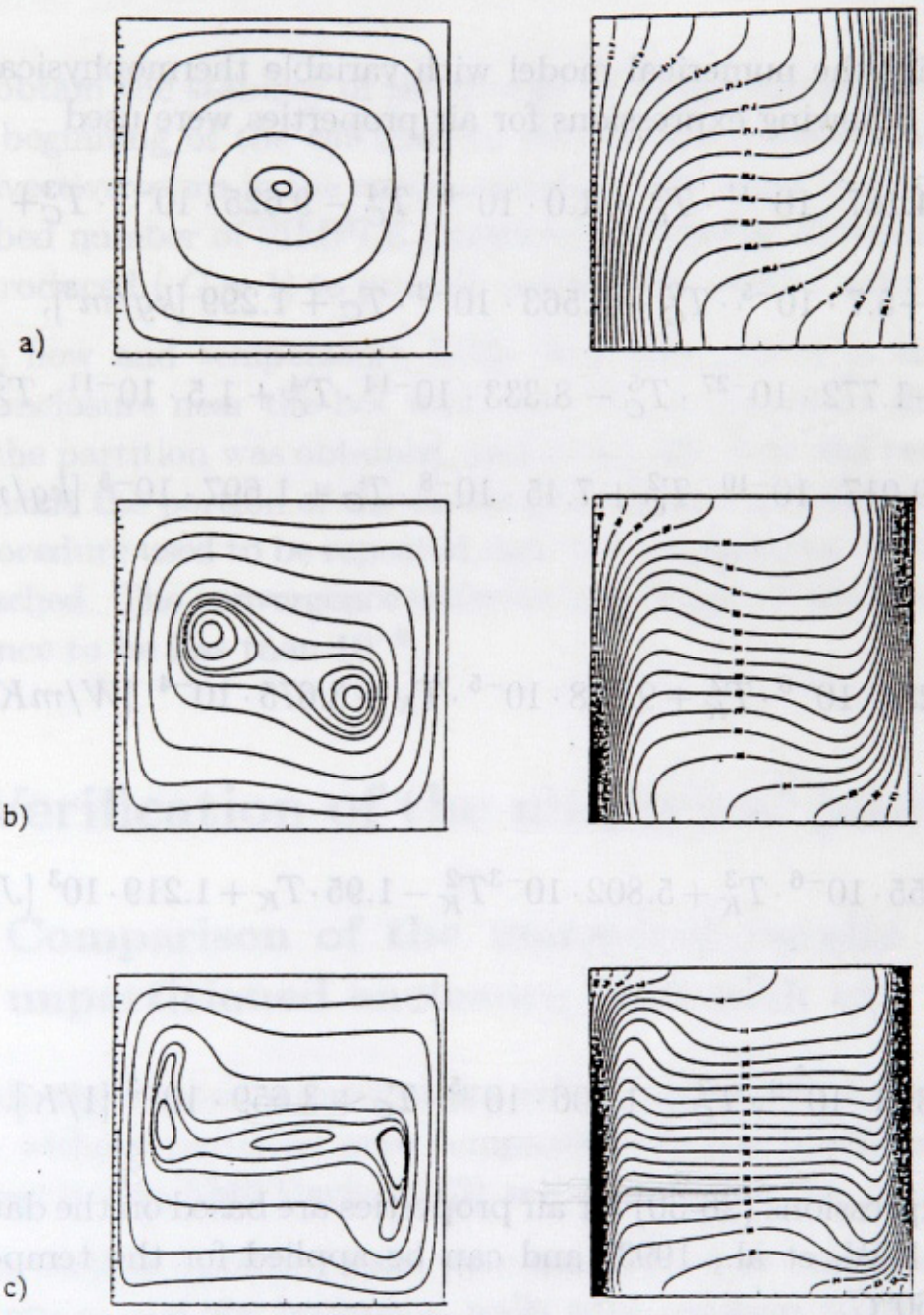

Fig. 3. Streamlines and isoterms for the enclosure without partition with air as a working fluid (Pr = 0.71)
a) $Ra = 10^4$, b) $Ra = 10^5$, c) $Ra = 10^6$.

The average Nusselt numbers are compared in Table 1 where the results from (de Vahl Davis, 1983), (Hortmann M., et al. 1989), and this paper are presented in the first, second and third rows, respectively.

Table 1. Comparison of the average Nusselt numbers for the enclosure without partition with air as a working fluid (Pr = 0.71).

Ra	10^4	10^5	10^6
de Vahl Davis, 1983	2.243	4.519	9.799
Hortmann M. et al., 1989	2.24475	4.52164	8.82513
Presented results	2.256	4.549	9.068

The greatest discrepancy between the average Nusselt numbers is for $Ra = 10^6$ but it is not more than 2.7% (between rows 2 and 3). The central difference scheme was introduced after 800 SIMPLE iterations for $Ra = 10^4$ and $Ra = 10^5$ (by assuming of $G = 1$ instead of $G = 0$). The calculation was stopped after 2500 iterations (see Fig. 4 a).

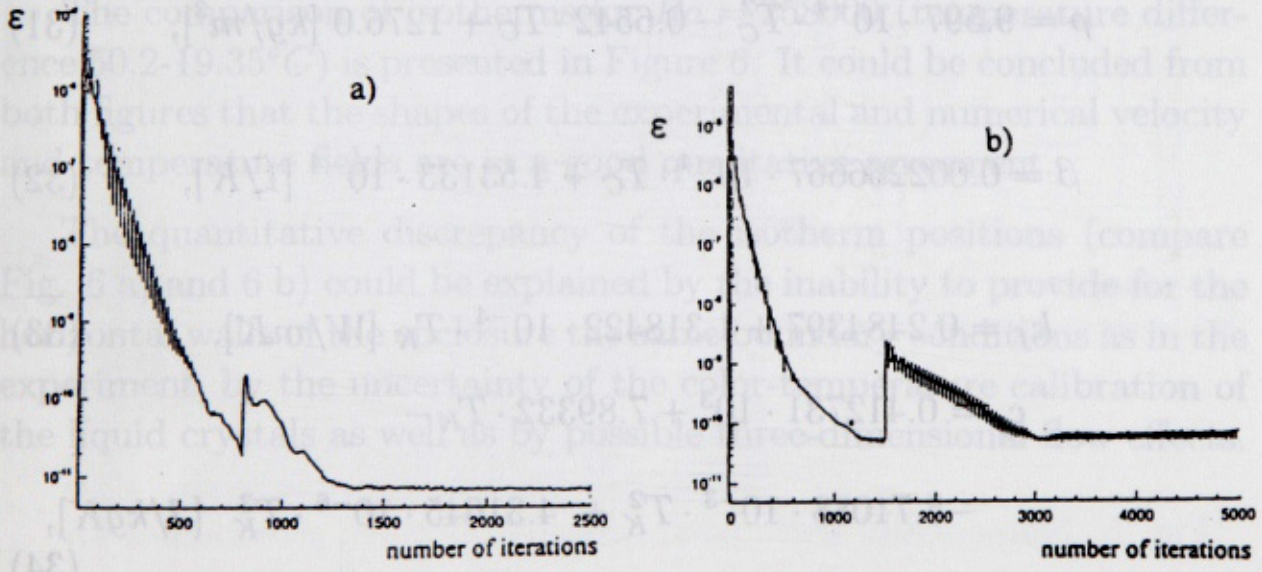

Fig. 4. Decrease of error (average mass imbalance) for a) $Ra = 10^4$, b) $Ra = 10^6$.

In the case of $Ra = 10^6$ the central difference scheme was introduced after 1500 iterations (with the factor G being changed from 0 to 0.6 - hence, not a complete central difference scheme) and calculation was stopped after 5000 iterations (see Fig. 4 b).

All the calculations were performed at the DEC 5000 work-station.

3.2 Results for the partitioned enclosure filled with glycerol

As another set of data, the experimental results from (D. Čučković - Džodžo et al., 1996 and D. Čučković-Džodžo, 1996) were used to verify the numerical model which takes into account the dependence of the thermophysical properties on temperature. Thermochromic liquid crystals and Plexiglas particles were used to visualize the temperature and velocity fields experimentally in the partitioned enclosure filled with glycerol (see Fig. 1). In this paper, the thermophysical properties of the glycerol were considered as being variable. They were specified as functions of temperature as follows

$$\rho = 9.597 \cdot 10^{-4} \cdot T_C^2 - 0.6542 \cdot T_C + 1276.0 \; [kg/m^3], \tag{31}$$

$$\beta = 0.002266667 \cdot 10^{-4} \cdot T_C + 4.53133 \cdot 10^{-4} \; [1/K], \tag{32}$$

$$k_f = 0.2484397 + 1.318422 \cdot 10^{-4} \cdot T_K \; [W/mK], \tag{33}$$

$$c_p = 0.412731 \cdot 10^3 + 7.89332 \cdot T_K - \\ -5.71088 \cdot 10^{-3} \cdot T_K^2 + \; 4.31645 \cdot 10^{-6} \cdot T_K^3 \; [J/kgK], \tag{34}$$

$$\mu = -1.63289 \cdot 10^{-8} \cdot T_C^5 + 4.129 \cdot 10^{-6} \cdot T_C^4 - 4.238 \cdot 10^{-4} \cdot T_C^3 + \\ +0.02241 \cdot T_C^2 - 0.62486 \cdot T_C + 7.6358 \; [kg/ms], \tag{35}$$

where T_C and T_K are temperatures in ^oC and K, respectively. The equations for the density, dynamic viscosity, and coefficient of the volumetric expansion were obtained experimentally (Džodžo,1991) while the curves for the coefficient of the conductivity and specific heat of glycerol were taken from (Toloukin Y. S. et al. ed., 1970) and (Toulokian Y.S. and Makita T., ed. 1970), respectively. Expressions can be applied for temperatures between 20-60^oC. The thermal conductivity of the plexiglas partition is assumed to be $k_p = 0.195\ W/mK$.

The numerically and experimentally obtained streamlines for $Ra = 96000$ and $Ra = 364000$ (temperature differences 38^oC-20^oC and 55.3-20.1^oC, resp.) are presented in Figure 5. By comparing Figures 5 a) and 5 b) it could be concluded that the increase of the Ra numbers brings forth an upward and downward shifting of the centers of the vortexes towards the horizontal axis in the hot and cold portion of the enclosure, respectively. The decrease of the thickness of the boundary layers for higher Ra numbers could be an explanation for the varying positions of the centers of the vortexes in the hot and cold halves of the enclosures. For the highest Ra numbers (Fig. 5 b) the small thickness of the boundary layers does not affect the positions of the vortex centers so that they are almost at the horizontal axis of the enclosure.

The comparison of isotherms for $Ra = 258000$ (temperature difference 50.2-19.35^oC) is presented in Figure 6. It could be concluded from both figures that the shapes of the experimental and numerical velocity and temperature fields are in a good qualitative agreement.

The quantitative discrepancy of the isotherm positions (compare Fig. 6 a) and 6 b) could be explained by the inability to provide for the horizontal walls of the enclosure the same boundary conditions as in the experiment, by the uncertainty of the color-temperature calibration of the liquid crystals as well as by possible three-dimensional flow effects.

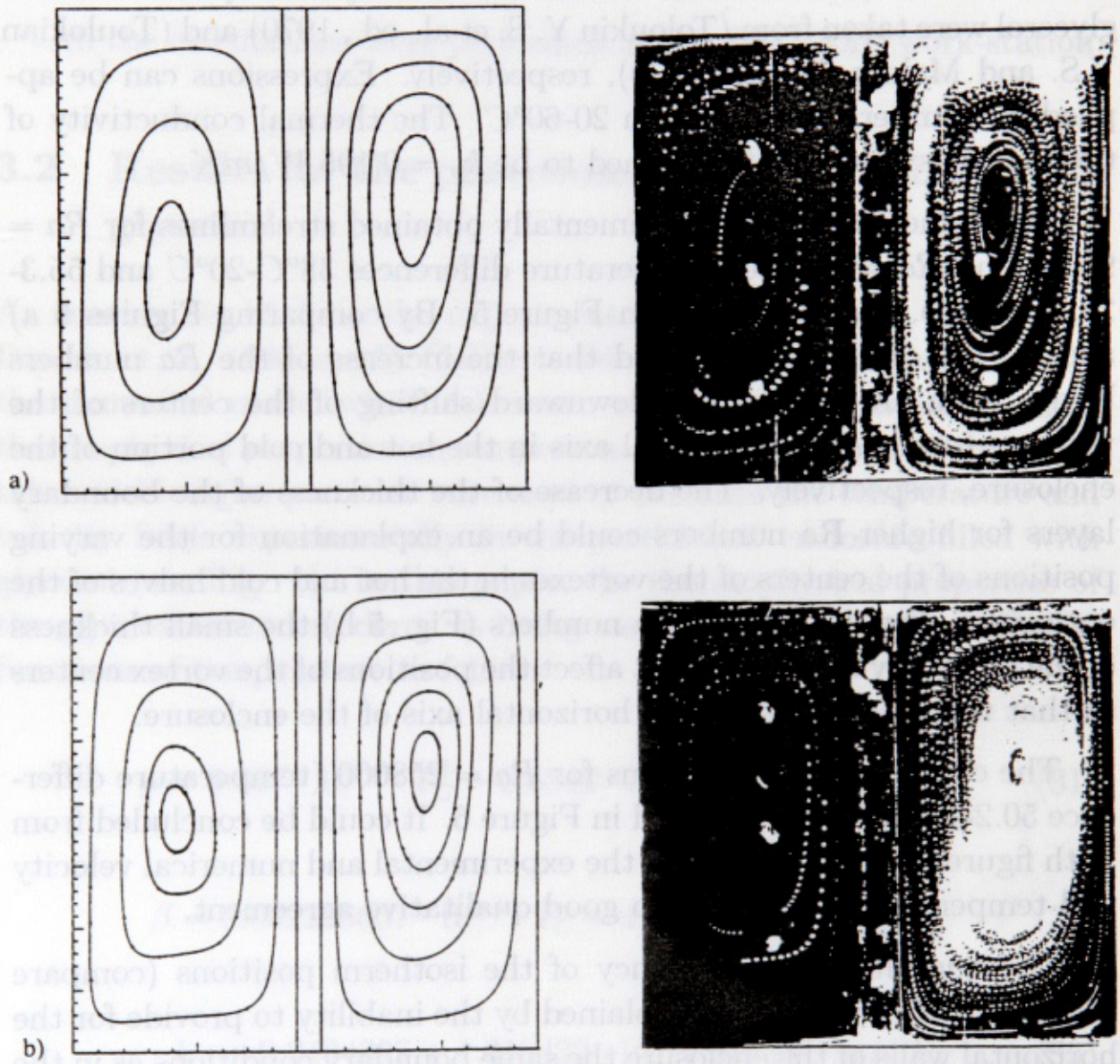

Fig. 5. Numerically and experimentally obtained streamlines for the enclosure with partition and glycerol as a working fluid

a) $T_h = 38^oC$ and $T_c = 20^oC$ (Pr = 5100, $Ra = 96000$),

b) $T_h = 55.3^oC$ and $T_c = 20.1^oC$ (Pr = 2700, $Ra = 364000$).

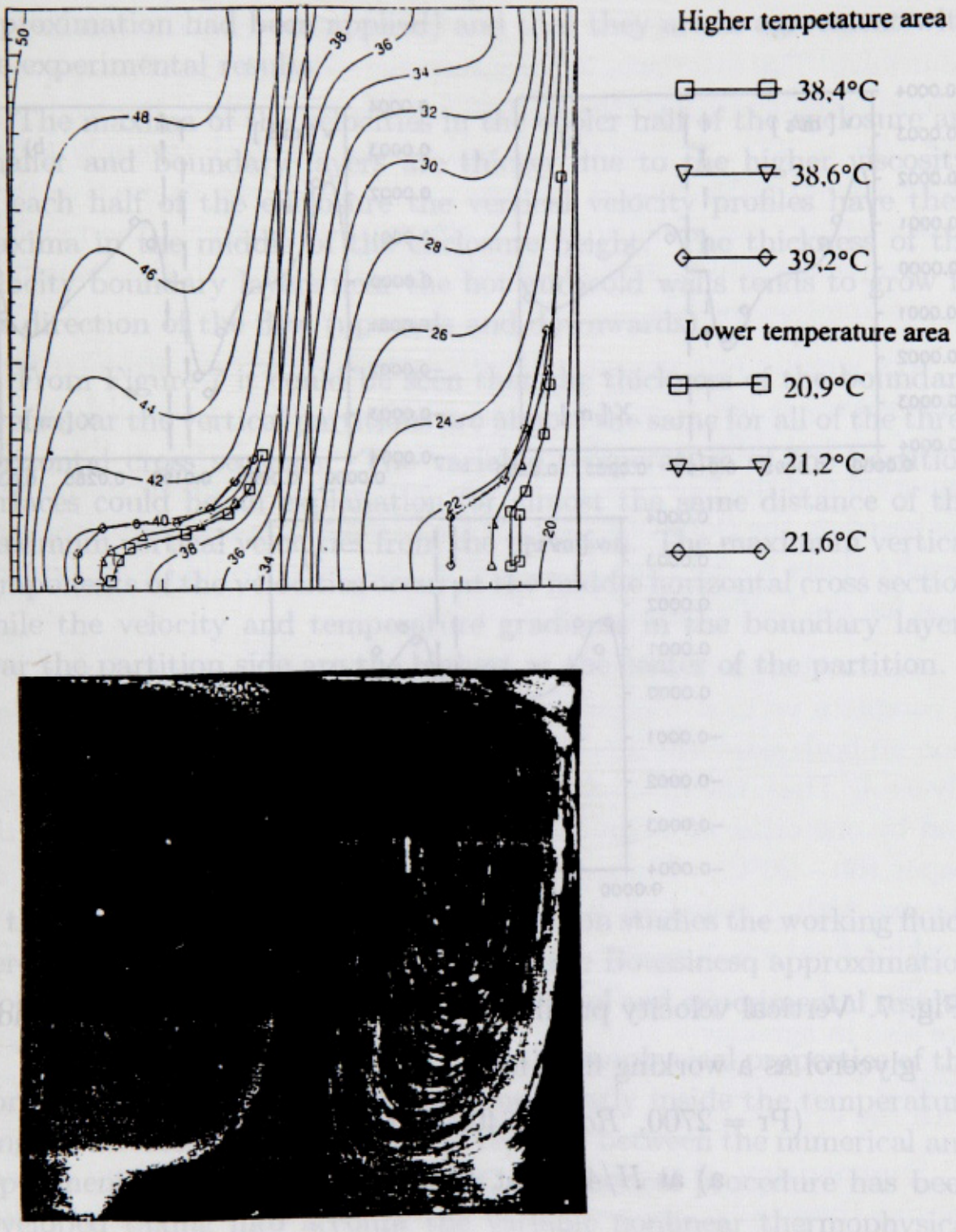

Fig. 6. Numerically and experimentally obtained isoterms for the enclosure with partition and glycerol as a working fluid for $T_h = 50.2°C$ and $T_c = 19.35°C$ (Pr = 3300, $Ra = 258000$).

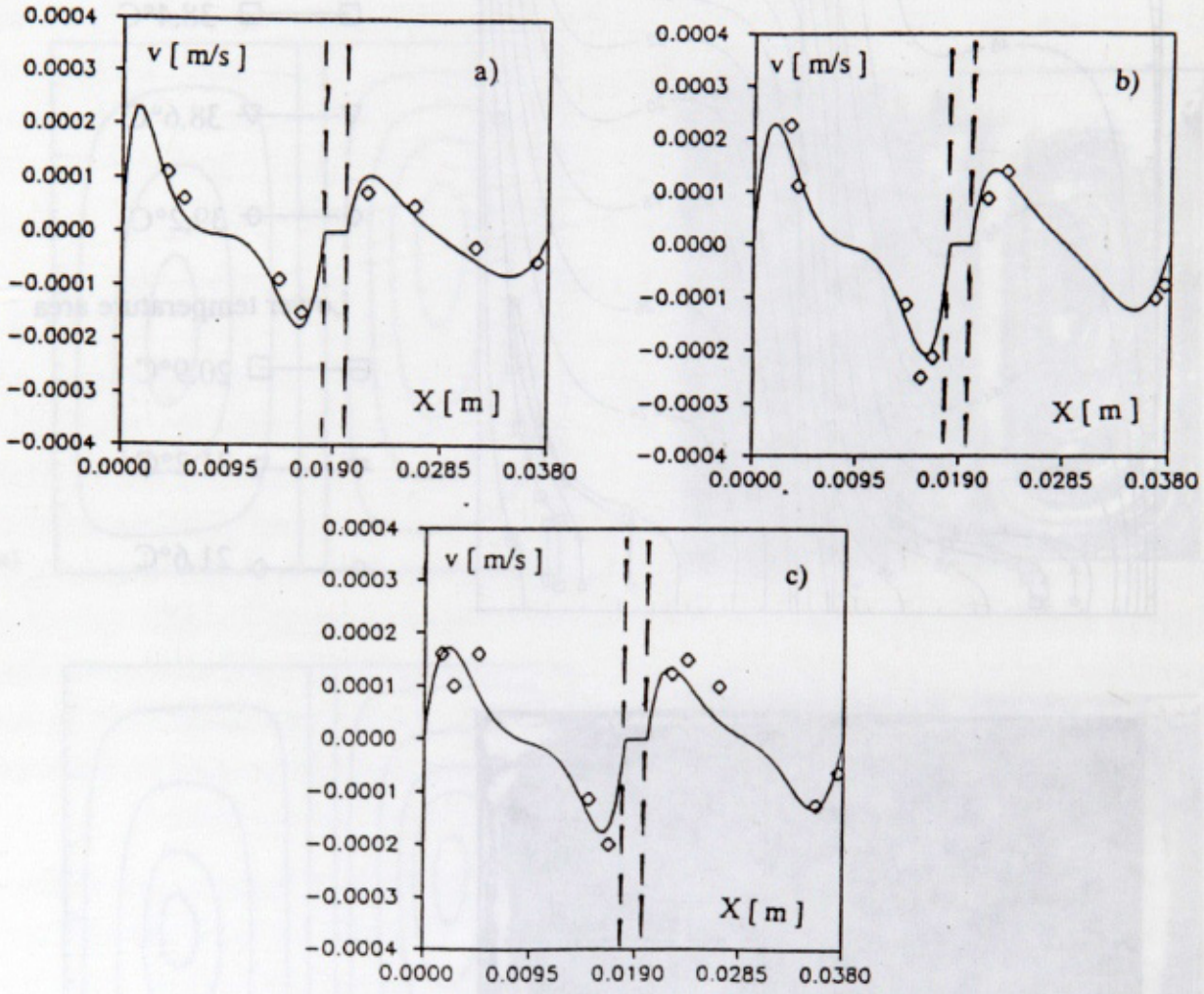

Fig. 7. Vertical velocity profiles in the enclosure with partition and glycerol as a working fluid for $T_h = 55.3^oC$ and $T_c = 20.1^oC$ (Pr = 2700, $Ra = 364000$) at different hights a) at $H/4$, b) at $H/2$, c) at $3H/4$.

In Figure 7, the numerically obtained vertical components of the velocities at various horizontal planes (solid lines) could be compared with the experimental results (symbols) for $Ra = 364000$ (temperature difference 55.3-20.1^oC). To note is that the numerically obtained velocity

profiles are not symmetrical (as they would have been if the Boussinesq approximation had been applied) and that they are in agreement with the experimental results.

The maxima of the velocities in the cooler half of the enclosure are smaller and boundary layers are thicker due to the higher viscosity. In each half of the enclosure the vertical velocity profiles have their maxima in the middle of the enclosure height. The thickness of the velocity boundary layers near the hot and cold walls tends to grow in the direction of the flow (upwards and downwards).

From Figure 7 it could be seen that the thickness of the boundary layers near the vertical partitions are almost the same for all of the three horizontal cross sections. The variable temperature of the partition surfaces could be an explanation for almost the same distance of the maximum vertical velocities from the partition. The maximum vertical components of the velocities occur at the middle horizontal cross section while the velocity and temperature gradients in the boundary layers near the partition side are the highest at the center of the partition.

4 Conclusions

In the most of the previous natural convection studies the working fluids were air or water and the application of the Boussinesq approximation produced no difference between the numerical and experimental results.

This is, however, not the case if the thermophysical properties of the working fluids vary drastically and nonlinearly inside the temperature range of interest. To reduce the discrepancy between the numerical and experimental results, for such fluids, a numerical procedure has been developed taking into account the variable nonlinear thermophysical properties of the working fluid.

The details of the developed numerical procedure are presented in the paper. The verification of the procedure has been performed by comparing the results obtained with the available natural convection numerical bench mark solutions (for air as a working fluid) as well as

with the experimental results (for glycerol as a working fluid).

The results for air are in a good agreement with the bench mark solutions. The maximum discrepancy between the calculated average Nusselt numbers is not greater than 2.7% for the highest Rayleigh number ($Ra = 10^6$). It might be based on the inability to apply a complete second order central difference scheme for the convective terms in the energy equation or on the effects of the varying thermophysical properties which were not taken into account with the Boussinesq approximation models.

For smaller temperature differences ($Ra = 10^5$ and $Ra = 10^4$) the discrepancy is less than 0.6%. The ability to apply a complete second order central difference scheme for the convective terms in the energy equation and the fact that for smaller temperature differences the models based on the Boussinesq approximation are supposed to produce the results closer to the ones developed in this paper could be an explanation for the better agreement obtained.

As another example the conjugate heat transfer in an enclosure with a complete vertical conducting partition and laminar natural convection on both sides was investigated numerically. The working fluid was glycerol. Thus, the dynamic viscosity of the glycerol varies nonlinearly and by one order of magnitude between the temperatures used in this paper (60 - 20^oC). Numerically obtained velocity profiles for the enclosure with a complete conductive vertical partition and glycerol as working fluid are in a close agreement with the experimental ones. The maxima of the velocity profiles and thickness of the boundary layers are also in agreement with the experiments. The numerically obtained temperature fields are qualitatively (shapes of isotherms) in agreement with the experiments.

Summarizing, the developed numerical model taking into account varying thermophysical properties of the fluid can in some cases reduce the discrepancy between the numerical and experimental results and thus produce more accurate results than models based on the Boussinesq approximation.

Acknowledgment. The authors are grateful to Prof. M.J. Braun

(The University of Akron, Mechanical Eng. Dept.) who gave us the opportunity to finish this work by allocating the laboratory equipment and computer facilities. The partial financial support from the Faculty research grant No: 2-07289 (The University of Akron) allocated to M. Džodžo is acknowledged as well.

Nomenclature

c_p - specific heat of the fluid $[J/kgK]$,

g - acceleration due to gravity $[m/s^2]$,

H- high of the enclosure $(H = W)$ $[m^2]$,

k_f - thermal conductivity of the fluid $[W/mK]$,

k_p - thermal conductivity of the partition $[W/mK]$,

p - pressure $[N/m2]$,

$\mathrm{Pr} = \frac{\nu}{\alpha}$ Prandtl number,

$Ra = \frac{g\beta(T_h - T_c)W^3}{\nu\alpha}$ Rayleigh number,

T - temperature $[^oC]$,

V - velocity vector $[m/s]$,

u - velocity along x $[m/s]$,

v - velocity along y $[m/s]$,

U or $V_{(P,W,E,N,S)}$ - velocities at the centers of the control volume cells,

U or $V_{(w,e,n,s)}$ - velocities at the faces of the control volume cells,

U or $V_{(sw,\ se,nw,ne)}$ - velocities at the corners of the control volume cells (for example $V_{ne} = (V_P + V_E + V_N + V_{NE})/4$),

W - width of the enclosure $[m]$,

N.B.: physical properties , and were taken for mean fluid temperature in the enclosure $(T_o = (T_h + T_c)\ /2)$ to calculate Ra and Pr.

Greek symbols

α- thermal diffusivity $[m^2/s]$,

$\alpha_{(u,v,p,T)}$ - underrelaxation factors,

β - thermal expansion coefficient of the fluid $[1/K]$,

ρ - density of the fluid $[kg/m^2]$,

μ - dynamics viscosity of the fluid $[kg/ms]$,

ν-cinematics viscosity of the fluid $[m^2/s]$.

References

[1] S. Acharya and C.H. Tsang, Natural convection in a fully partitioned, inclined enclosure, Numerical Heat Transfer, (1985), Vol. 8, 407-428.

[2] R. Andersen and A. Bejan, Heat transfer trough single and double vertical walls in natural convection: theory and experiment, Int. J. Heat Mass Transfer, (1981), Vol. 24, 1611-1620.

[3] M. Ciofalo and T.G. Karayiannis, Natural convection heat transfer in a partially - or completely-partitioned vertical rectangular enclosure, Int. J. Heat Mass Transfer, (1991), Vol. 34, No. 1., 167-179.

[4] D. Čučović-Džodžo, M. Džodžo and M. Pavlovi´c, Visualization of Laminar Natural Convection in a Cubical Enclosure with Partition, Fluids Engineering Division Summer Meeting, San Diego, July 7-11, 1996, Volume 4, 225-230.

[5] D. Čučović-Džodžo, Effects of Heat Conducting Partition on Laminar Natural Convection in an Enclosure, M. Sc. thesis, Faculty of Mechanical Engineering, The University of Belgrade, 1996.

[6] G. de Vahl Davis, Natural convection of air in a square Cavity: A Bench Mark Numerical Solution, Int. J. Numer. Meth. Fluids, (1983), Vol. 3, 249-264.

[7] G. de Vahl Davis and I.P. Jones, Natural convection in a square cavity: a comparison exercise, Int. J. Numer. Meth. Fluids, (1983), Vol. 3, 227-248.

[8] D. Duxbury, An Interferometric Study of Natural Convection in Enclosed Plane Air Layers with Complete and Partial Central Vertical Divisions, Ph.D. Thesis, University of Salford, (1979).

[9] M. Džodžo, Laminar Natural Convection in some Enclosures of Arbitrary cross Section Ph.D. Thesis, Faculty of Mechanical Engineering, The University of Belgrade, 1991.

[10] M. Džodžo, Visualization of laminar natural convection in romb-shaped enclosures by means of liquid crystals, ed. Sideman S., Hijikata K., Yang W. J., Imaging in Transport Processes, Begel House Publishers, (1993), Chapter 15, 183-193.

[11] W. J. Hilller , St. Koch and T.A. Kowalewski and F. Stella, Onset of natural convection in a cube, Int. J. Heat Mass Transfer, (1993), Vol. 36, No. 13, 3251-3263 .

[12] M. Hortmann , M. Peric , G. Scheuerer, Finite Volume Multigrid Prediction of Laminar Natural Convection: Bench-Mark Solutions, Int. J. Numer. Meth. Fluids, (1990), Vol. 11, 189-207.

[13] A. Kangni, R.B. Yedder and E. Bilgen, Natural convection and conduction in enclosures with multiple vertical partitions, Int. J. Heat Mass Transfer, (1991), Vol. 34, No. 11, 2819-2824.

[14] T.G. Karayiannis and M. Ciofalo and G. Barbaro, On natural convection in a single and two zone rectangular enclosure, Int. J. Heat Mass Transfer, (1992), Vol. 35, No. 7, 1645-1657.

[15] P.K. Khosla , S.G. Rubin, A diagonally dominant second-order accurate implicit scheme, Computers and Fluids, (1974),Vol. 2, 207-209.

[16] M. Mamou, M. Hasnaoui , P. Vasseur , and E. Bilgen, Natural convection heat transfer in inclined enclosures with multiple con-

ducting solid partitions, Numerical Heat Transfer, (1994),Part A: Applications, Vol. 25, 295-315.

[17] H. Nakamura , Y. Asako and T. Hirata, Natural convection and thermal radiation in enclosures with partition plate, Trans. JSME, (1984), Ser. B.50, 2647-2654.

[18] T. Nishimura, M. Shiraishi, F. Nagasawa and Y. Kawamura, Natural convection heat transfer in enclosures with multiple vertical partitions, Int. J. Heat Mass Transfer, (1988), Vol. 31, No 8, 1679-1686.

[19] S.V. Patankar, D.B. Spalding, A Calculation Procedure for Heat, Mass and Momentum Transfer in Three-Dimensional Parabolic Flows, Int. J. Heat Mass Transfer, (1972) Vol. 15, 1787-1806.

[20] S.V. Patankar, Numerical heat transfer and fluid flow, McGraw-Hill, New York, (1980).

[21] M. Peric, A Finite Volume Method for the Prediction of Three-Dimensional Fluid Flow in Complex Ducts, Ph.D. Thesis, University of London, (1985)

[22] C.M. Rhie, A numerical study of the flow past an isolated airfoil with separation, Ph.D. Thesis, University of Illinois, Urbana-Champaign, (1981)

[23] F.W. Schmidt , R.E. Henderson , C.H. Wolgemuth, Introduction to thermal sciences, Thermodynamics, Fluid Dynamics, Heat Transfer, John Wiley & Sons, Inc, (1993)

[24] H.L. Stone, Iterative Solution of Implicit Approximations of Multidimensional Partial Differential Equations, SIAM J. Num. Anal., (1968), Vol. 5. No 3, September 1968, 530-558.

[25] T.W. Tong and F.M. Gerner, Natural convection in partitioned air-filled rectangular enclosures, Int. Comm. Heat Mass Transfer, (1986), Vol. 13, 99-108.

[26] Y.S. Toulokian, P.E. Liley , S.C. Saxena (editors), Thermophysical Properties of Matter, The TPRC Data Series, Vol. 3, THERMAL CONDUCTIVITY Nonmetallic Liquids and Gases, IFI/Plenum, New York-Washington, (1970)

[27] Y.S. Toulokian, T. Makita (editors), Thermophysical Properties of Matter, The TPRC Data Series, Vol. 6, SPECIFIC HEAT Nonmetallic Liquids and Gases, IFI/Plenum, New York-Washington, (1970).

Dušanka M. Čučković-Džodžo
2846 Riviera Drive Apt. D
Akron, OH 44325, USA

Milorad B. Džodžo
Westinghouse Science and Technology Center
Pittsburgh, PA,USA

Miloš D. Pavlović
Faculty of Mechanical Engineering
University of Belgrade
Belgrade, Yugoslavia

Matematički model i numeričko rešenje za konjugovani prenos toplote u izdeljenom okruženju za fluide sa promenljivim nelinearnim termodinamičkim svojstvima

Lamilarna prirodna konvekcija u okruženju izdeljenom kompletnim vertikalnim provodnim particijama je studirana numerički pomoću stacionarnog dvodimenzijskog modela. Korišćene su jednačine za fluide različite gustine i različitih termofizičkih svojstava. Razvijena numerička procedura je verifikovana uporedjivanjem rezultata za vazduh i glicerin.

Kako procedura u obzir uzima nelinearnu zavisnost termofizičkih svojstava glicerina (posebno viskoznosti) dobijeno je bolje slaganje sa eksperimentalnim rezultatima.